Neuromodulation: Technology at the Neural Interface

Received: April 25, 2022 Revised: August 2, 2022 Accepted: August 15, 2022

https://doi.org/10.1016/j.neurom.2022.08.450

High-Definition Transcranial Infraslow Pink-Noise Stimulation Can Influence Functional and Effective Cortical Connectivity in Individuals With Chronic Low Back Pain: A Pilot Randomized Placebo-Controlled Study

Divya Bharatkumar Adhia, PhD[1,5]; Ramakrishnan Mani, PhD[2,5]; John N. J. Reynolds, PhD[3]; Matthew Hall, PGDipSci[1]; Sven Vanneste, PhD[4]; Dirk De Ridder, PhD[1,5]

ABSTRACT

Introduction: Pain can be regarded as an emergent property of multiple interacting, dynamically changing brain networks and thus needs a targeted treatment approach. A novel high-definition transcranial infraslow pink-noise stimulation (HD-tIPNS) technique was developed to modulate the key hubs of the three main nociceptive pathways simultaneously, ie, the pregenual anterior cingulate cortex (pgACC) (descending inhibitory pathway), the dorsal anterior cingulate cortex (dACC) (medial nociceptive pathway), and both somatosensory cortices (S1) (lateral nociceptive pathway). This study aimed to evaluate safety and verify whether a single session of HD-tIPNS may disrupt functional and effective connectivity between targeted cortical regions.

Materials and Methods: A pilot double-blind randomized two-arm placebo-controlled parallel trial was conducted. Participants (N = 30) with chronic low back pain were equally randomized to receive a single session of either sham stimulation or HD-tIPNS (targeting the pgACC, dACC, and bilateral S1). Primary outcomes included safety and electroencephalographic measures, and secondary outcomes included pain measures, collected after treatment. A Mann-Whitney *U* test was used to compare between-group differences in percentage changes with baseline for each outcome measures. A Wilcoxon signed-rank test was used to identify difference in effective connectivity measure before and after HD-tIPNS.

Results: No serious adverse events were reported. A significant decrease in instantaneous functional connectivity was noted between the pgACC and dACC ($U = 47.0$, $Z = -2.72$, $p = 0.007$) and the pgACC and left S1 ($U = 41.0$, $Z = -2.97$, $p = 0.003$) in the infraslow band after HD-tIPNS when compared with sham stimulation. A significant decrease in instantaneous effective connectivity was noted in the direction of the dACC to the pgACC ($Z = -2.10$, $p = 0.035$), in the infraslow band after HD-tIPNS when compared with baseline. No changes in clinical pain measures were detected.

Conclusions: HD-tIPNS can safely modulate the functional and effective connectivity between targeted pain-related cortical hubs. Further studies are warranted to evaluate whether repeated exposures to HD-tIPNS can incur clinical benefits through inducing changes in functional and effective connectivity at targeted cortical regions.

Clinical Trial Registration: The Clinicaltrials.gov registration number for the study is ACTRN12621001438842.

Keywords: Chronic low back pain, effective connectivity, functional connectivity, randomized placebo-controlled trial, transcranial random noise stimulation

Address correspondence to: Divya Bharatkumar Adhia, Department of Surgical Sciences, Otago Medical School, University of Otago, PO Box 56, Dunedin 9054, Otago, New Zealand. Email: divya.adhia@otago.ac.nz

[1] Department of Surgical Sciences, Dunedin School of Medicine, University of Otago, Dunedin, Otago, New Zealand;
[2] School of Physiotherapy, Centre for Health, Activity and Rehabilitation Research, University of Otago, Dunedin, Otago, New Zealand;
[3] Department of Anatomy and the Brain Health Research Centre, School of Biomedical Sciences, University of Otago, Dunedin, Otago, New Zealand;
[4] School of Psychology, Global Brain Health Institute, Trinity College Dublin, Dublin, Ireland; and
[5] Pain@Otago Research Theme, School of Physiotherapy, University of Otago, Dunedin, Otago, New Zealand

For more information on author guidelines, an explanation of our peer review process, and conflict of interest informed consent policies, please see the journal's Guide for Authors.

Source(s) of financial support: This work was supported by New Zealand Health Research Council (20/618), Healthcare Otago Charitable Trust, Brain Health Research Centre, and a gift from John Ward. The funding bodies were not involved in study conceptualization or design, data collection/analysis/interpretation, in the writing of the report, and in the decision to submit the article for publication.

Conflict of Interest: The authors reported no conflict of interests.

INTRODUCTION

The human brain is a complex adaptive system.[1,2] Over time, driven by the forces of evolution, it has progressively increased in complexity, with a primary goal of reducing the inherent uncertainty present in an ever-changing environment.[3] To qualify as a complex adaptive system, a system must fulfil two criteria.[4] It needs to express a small-world topology and must embed noise,[4] permitting the system to be adaptive, in contrast to both a rigid lattice (regular) and random network.[5] An intermediate structure between these extremes (regular vs random) is characterized by a small-world topology, which permits flexibility and adaptation to changing environments through variability. All complex adaptive systems share defining characteristics. One of the fundamental characteristics of these systems is emergence, meaning that the whole is more than the sum of its components. Emergence is a process whereby features, patterns, and regularities arise in a system through interactions among the components of the systems, which themselves do not exhibit such features.[6] For example, the randomly assembled components of a car do not independently form a vehicle capable of automation. However, when they are assembled and connected in a precise way, automotion emerges from the car, as a complex (in this case, nonadaptive) system.

Pain can be regarded as an emergent property of multiple interacting and dynamically changing brain networks.[7] Three major networks in pain have been described and can be anatomically and symptomatically dissociated into three distinct but interacting pathways: a lateral "painfulness" pathway, a medial "suffering" pathway, and a descending "pain inhibitory" pathway.[7–10] The key cortical structures involved include the primary somatosensory cortex (S1), dorsal anterior cingulate cortex (dACC), and pregenual anterior cingulate cortex (pgACC), respectively. Recent evidence suggests that alterations in functional connectivity patterns between the pain processing regions (pgACC, dACC, and S1) are critical for maintaining chronic pain and are associated with its clinical and psychologic outcomes.[11–20]

One can attempt to disrupt abnormal functional connectivity patterns through neuromodulation, including noninvasive transcranial electrical stimulation and implantable devices.[21–23] Recently, we have proposed that one way of breaking connectivity may be through applying pink-noise stimulation,[24,25] which mimics the temporal structure of brain function (because of its structure).[26,27] Resting-state connectivity in the brain is most commonly studied with functional magnetic resonance imaging (fMRI); this is also true in pain research.[28–31] The fMRI blood oxygen level–dependent signal correlates with infraslow electroencephalography (EEG) signals[32,33] and may represent astrocytic calcium waves, essential in synchronizing neural activity.[34–37] Thus, it can be envisaged that combining infraslow and pink noise in one stimulation design may benefit people with chronic pain by disrupting pathological functional and effective connectivity. A first step in the translation of this concept is to verify whether this basic assumption is correct, in that this stimulation design can disrupt pathological connectivity in people with chronic pain.

On the basis of network science, used to study complex adaptive systems, it has become clear that random attacks on brain networks cannot disrupt a network[38] and consequently the emergent properties of the network[22]—in this case, pain. Therefore, a targeted attack[38] on the main hubs of the three networks involved in pain is more likely to disrupt pathological connectivity and exert a beneficial effect.[22] This agrees with a meta-analysis on deep brain stimulation for pain that shows that multitarget implants yield better outcomes than single target stimulation, especially if both lateral and descending pain inhibitory pathways are jointly targeted.[39]

Consequently, a targeted, high-definition transcranial stimulation technique was developed to modulate the key hubs of the three main pain pathways simultaneously, ie, the pgACC (descending pain inhibitory pathway), the dACC (medial pain pathway), and bilateral S1 (lateral pain pathway), using pink noise embedded in an infraslow component. This study aimed to evaluate safety and verify whether a single session of this novel approach may disrupt functional and effective connectivity between the targeted cortical regions.

MATERIALS AND METHODS

Registration and Ethical Approval

This study was prospectively registered in the Australian and New Zealand Clinical Trials Registry (https://www.anzctr.org.au/Trial/Registration/TrialReview.aspx?id=382818; registration number: ACTRN12621001438842; date of registration: October 25, 2021). This pilot study was conducted according to the 1964 Declaration of Helsinki ethical standards. Ethical approval was obtained from the New Zealand Health and Disability Ethics Committee (Ethical approval number: 20/NTB/67). All participants provided written informed consent before study enrolment.

Study Design

This was a pilot double-blind randomized placebo-controlled parallel trial with two intervention arms, with the outcome measures collected at baseline and immediately after intervention.

Randomization

A research administrator, not involved in treatment or assessment procedures, randomized eligible volunteers using an open-access randomization software program, to one of the two intervention arms (on a 1:1 basis):

- Group 1: High-definition transcranial infraslow pink-noise stimulation (HD-tIPNS)
- Group 2: Sham stimulation

The randomization schedule was concealed in sequentially numbered, sealed opaque envelopes and provided to participants at their baseline measurement.

Blinding

The participants and the outcome assessor were blinded to group allocation. The success of blinding was assessed after the completion of the intervention. The participant and the outcome assessor were asked, "What type of treatment do you believe that

you/the participant received?" and were required to choose between three options: active, sham, or do not know. The confidence in their judgment was also assessed on an 11-point numeric rating scale (NRS; 0 = *not at all confident* to 10 = *extremely confident*), with the reason for their judgment being noted and whether the intervention was revealed to them. Unblinding was permissible only in the case of an adverse event or any unexpected event.

Study Setting

This study was conducted in the Department of Surgical Sciences laboratory, Dunedin School of Medicine, Dunedin Hospital, New Zealand.

Participants and Eligibility Criteria

An experienced researcher with a musculoskeletal physiotherapy background screened all the volunteers for eligibility.

Inclusion Criteria

The inclusion criteria were as follows: capable of understanding and signing an informed consent form, age from 18 to 75 years on the day of the consent, pain in the lower back (the region between the 12th rib and gluteal fold) that occurs every day for ≥3 months, a score of >4 on an 11-point numeric pain rating scale[40] (NPRS, 0 = *no pain* to 10 = *worst pain imaginable*) in the past four weeks before enrolment, and a disability score of ≥5 on the Roland-Morris Disability Questionnaire.[41,42] These cutoff scores are used as an indication that chronic low back pain (CLBP) significantly affects daily functioning, are by the International Association of Study of Pain guidelines, and are in line with optimal Delphi definitions of low back pain prevalence.[41–45]

Exclusion Criteria

Participants with the following self-reported health conditions were excluded: inflammatory arthritis, undergoing any therapy from a health professional (eg, physiotherapist or chiropractor), recent soft tissue injuries of the back in the last three months, history of surgery to the back region, current intake of any centrally acting medications or intention of taking new medications on the treatment day, steroid injections to the back in the last six months, radicular pain and radiculopathy, history of neurologic diseases, unstable medical or psychiatric conditions, history of epilepsy or seizures, peripheral neuropathy, vascular disorders, substance abuse, dyslipidemia, cognitive impairments [dementia, post-traumatic stress disorders, Alzheimer disease; assessed as a score of <24 on the mini-mental status examination], history of uncontrolled/untreated hypertension, presence of any pacemaker or defibrillator or electronic/metal body implants (around the head/neck region), and recent or current pregnancy.

Recruitment and Study Enrolment

A total of 30 participants (n = 15/group) were recruited from the community, primarily through broadcasting in the public media (eg, newspapers and social media). Advertisement fliers were placed around a tertiary hospital, regional health care practices, and supermarkets. A recruitment email was sent to the local tertiary educational university/polytechnic staff and students to recruit a representative sample.

All volunteers completed an online screening questionnaire. Potential participants were contacted by a researcher with a health professional background (trained musculoskeletal physiotherapist) to undergo more screening over the phone to confirm eligibility before study enrolment. The study information sheet was emailed to eligible participants. Written informed consent was obtained before baseline testing. All participants completed questionnaires to capture demographics, clinical characteristics of CLBP, including presence of central sensitivity (Central Sensitization Inventory),[46,47] neuropathic pain quality (PainDETECT),[48] and psychologic measures (Depression, Anxiety, and Stress Scale,[49] Pain Catastrophizing Scale,[50,51] and Pain Vigilance and Awareness Questionnaire[52]).

Intervention Procedures

The intervention was administered for a single session of 30 minutes by a researcher experienced in noninvasive neuromodulation techniques. A battery-driven, wireless high-definition transcranial electrical stimulator (Starstim32, Neuroelectrics, Barcelona, Spain) with 32 independent current sources, permitting performance of multitarget stimulation,[53] was used to deliver stimulation while participants were comfortably and quietly seated. A total of 35 small electrodes (~4 cm^2) were placed on a standardized neoprene head cap, following the International 10–10 EEG electrode placement system to simultaneously target the pgACC, dACC, and S1. Care was taken to observe the principles of Tikanga Māori (correct protocols for Māori) when interacting with Māori participants, acknowledging that for Māori, the head is tapu (sacred).

For the active stimulation (group 1), the HD-tIPNS was delivered at a current strength of a maximum of 2 mA for 30 minutes, with 60-second ramp up and ramp down at the beginning and end of the stimulation session, with continuous stimulation in between. The pink-noise stimulation at a maximum current strength of 1 mA was superimposed on the infraslow (0.1 Hz sinusoidal) waveform of a current intensity of 1 mA (Fig. 1). The current strength at each electrode never exceeded the maximum safety limit of 2 mA (Fig. 1). The intervention dosage was based on the previous transcranial electrical stimulation studies[54–64] and followed safety guidelines.[65–67]

For the sham stimulation (group 2), the Actisham protocol created by Neuroelectrics was used to create an identical skin sensation to active stimulation.[68] The current was applied for 60-second ramp up and 60-second ramp down at the beginning and at the end, without any current for the remainder of the session. The duration of the sham session was like HD-tIPNS session, to blind the procedure appropriately. Participants in both groups were informed that they might or might not perceive any sensations during the stimulation treatment.

Montage optimizations for the active stimulation and the Actisham (Fig. 2) were performed using the Stimweaver algorithm by Neuroelectrics. The Stimweaver algorithm optimizes the E_n component of the E-field (ie, component of the E-field normal to the cortical surface), using the assumption of the lambda-E model for the interaction of the E-field with the neurons.[53,69,70] The algorithm finds the best montage for targeting regions by trying to minimize the least squares difference between the weighted target *En*-map and the weighted *En*-field distribution produced by the montage. For the purposes of this study, the parameters for the problem used to find the best montage were stimulation type, target (S1, pgACC, and dACC), electric field in target area (0.25 V/m excitatory), electrode type (PITRODE PISTIM, π cm^2 area, Ag/AgCl/gel electrode), maximum current any electrode (1.0 mA), maximum number of electrodes (n = 8), and other (10–10 standard head cap, 39 positions available). The standard safety constraint applied was

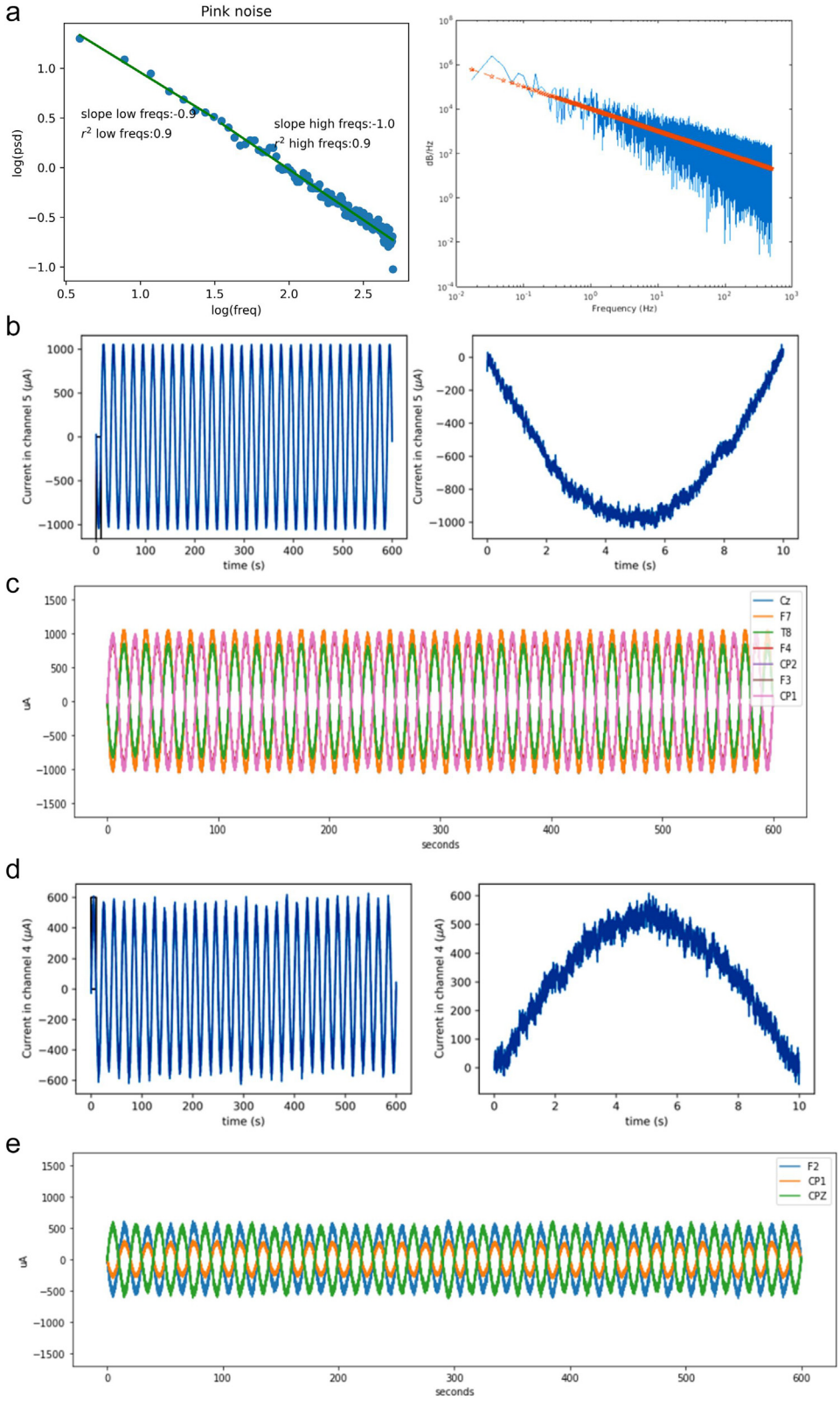

Figure 1. Infraslow pink-noise waveform details. Power spectral density profile of the (a) pink-noise component and the 1/f structure (ie, pink-noise power spectral density decreases with 1/f). Pink noise was nested on the infraslow (0.1 Hz) sinusoidal wave component for (b and c) the active treatment group and (d and e) the sham treatment group, respectively. For both groups, the waveforms were identical. The infraslow component lasts for 10 seconds (ie, 0.1 Hz), after which the phase is inverted. The pink-noise component has a maximum of 1 mA and follows a 1/f power-to-frequency structure. freq, frequency; psd, power spectral density. [Color figure can be viewed at www.neuromodulationjournal.org]

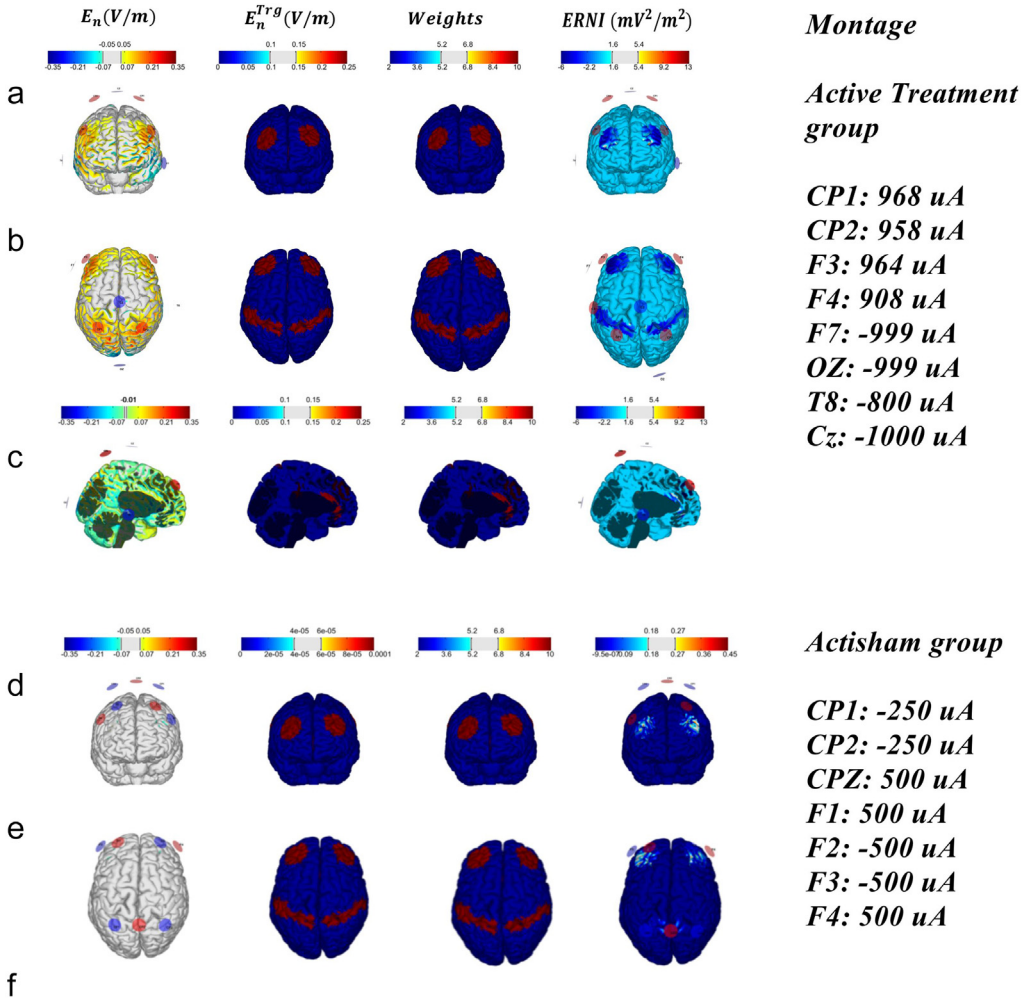

Montage	ERNI (mV^2/m^2)	WCC	$< E_n >$ on areas to excite
Active	-9860	0.49	0.043
Actisham	279.9	-0.0002	0.0004 (Ratio Active/Actisham = 121)

Figure 2. Montage optimization for the high-definition transcranial infraslow pink-noise stimulation and the Actisham intervention. This figure presents the optimization that was created using the Stimweaver software by Neuroelectrics for targeting the activity of the pgACC, dACC, and S1.[70] The S1 and pgACC targets were identified with the Neuroelectrics online target editor. The dACC was targeted through its connections with the DLPFC (center points with MNI coordinates: [32, 46, 30] and [−28, 42, 34]). The ROI for the DLPFC was selected through Neurosynth's (https://neurosynth.org/) functional connectivity calculation. Electrical currents at the targeted areas and the final montage used are presented for active treatment group (a: front view; b: top view; c: sagittal view) and the sham group (d: front view; e: top view; f: sagittal view), respectively. From left to right: Normal component of the E-field E_n (V/m), target E-field (V/m), target weight, and ERNI (mV^2/m^2) for gray matter. For the active group, the electrical current is delivered through eight of the 32 channels in a fractionated way, to optimize the current at the three targets in the brain, based on a computer simulation on a standard head model. The currents for each electrode are detailed in montage section (right column) for the active treatment group and the Actisham group, respectively. (g) The comparison of the E-field between groups shows an E_n of the active treatment group to be 121 times more than in the Actisham group. [Color figure can be viewed at www.neuromodulationjournal.org]

that the maximal total injected current into the brain at any given time was <3.8 mA. The last condition is imposed using a genetic algorithm that searches in electrode space for the constrained solution that better approximates the optimization objective function.[53]

The pgACC and S1 areas were directly created with the Neuroelectrics online target editor. The network of areas correlated with the dACC (Montreal Neurological Institute [MNI] coordinates [−4, 8, 36]) was obtained with Neurosynth initially and then limited to the dorsolateral prefrontal cortex (DLPFC) (10-mm radius circular areas centered in [32, 46, 30] and [−28, 42, 34] mm). The weights were set to the maximum value in all areas. The target E_n-field was set to 0.25 V/m. The rest of the cortex was set to a no-stimulation condition (E_n^{Target} = 0 V/m) with minimum weight. Optimizations were run for this target map up to a maximum of 12 electrodes in the montage. The target maps are shown in Figure 2 (second and third

columns). The eight-channel montage solution resulted in a good fit to the target map, with error relative to no intervention (ERNI) and weighted correlation coefficient (WCC) scores that are >96% of those obtained with an unconstrained number of electrodes: −9862 mV^2/mm^2 and 0.493, respectively. The distribution of the E_n component of the E-field is shown in Figure 2. The final montage and the currents per electrode used for the active stimulation were as follows:

CP1: 968 μA
CP2: 958 μA
F3: 964 μA
F4: 908 μA
F7: −999 μA
OZ: −999 μA
T8: −800 μA
Cz: −1000 μA
Total injected current (μA): 3798 μA
Maximum current at any electrode (μA): 1000 μA
Fitness function (ERNI): −9863.918 mV^2/m^2
Fitness function (ERNI) relative to full solution: 0.974

One adverse effect of the active stimulation condition can be localized itching at the electrode sites; hence, in the Actisham condition, the currents are configured to produce similar itching to the active condition, but very low cortical electric fields. This is achieved using the Stimweaver optimization algorithm, which now has the objective of a null or a very low electric field on target (ie, pgACC, dACC, and S1). The parameters for the problem were similar to those used for finding the best montage for the active stimulation group, except the electric field in the target area was constrained to 0.001 V/m. To minimize the trivial solution (all currents, set to 0), a minimum of 500 μA is imposed in one of the electrodes as an optimization constraint. The electrode set to this current is deemed informally the "itchy electrode" because its presence induces a sensation like that of active stimulation. The Actisham montage achieves a low En-field on target by maximizing current shunting through the skin, and it usually results in anodes and cathodes placed over the target in an alternating pattern. Because the target in this optimization consists of clusters of target areas, the algorithm we followed was adapted to this case: the target was divided into three clusters of regions, two comprised the dACC and pgACC in the left/right hemispheres and another one comprised the S1 region. The Actisham optimization algorithm was then run independently for the two clusters of regions. For each optimization, we defined a pool of electrodes consisting of the ones from the active montage over those regions, plus extra electrodes to guarantee a dense distribution of electrodes over the target (required for high shunting of current through the skin, which results in low E_n-field in the brain regions). The E_n-field distribution induced by all three montages is localized enough so that when all electrodes are present at the same time, the distribution over each target is not very different from the individual montages, thus ensuring that the combined montage is an effective Actisham montage for all target regions. The final montage and the currents per electrode used for the sham stimulation were as follows:

CP1: −250 μA
CP2: −250 μA
CPZ: 500 μA
F1: 500 μA
F2: −500 μA
F3: −500 μA
F4: 500 μA

This montage generates an average E_n-field in the target regions that is much lower than the one induced in the active montage (0.004 V/m in Actisham vs 0.043 V/m in the active montage) (Fig. 2d–g). The Actisham method of sham stimulation ensures double blinding and delivers similar peripheral nervous system (PNS) stimulation across conditions, so putative PNS effects will be present in both active and sham stimulation. The previous transcranial electrical stimulation studies[71] have used this sham procedure and have shown it to effectively blind participants to the stimulation condition because it can induce the same scalp sensations perceived during active stimulation, in terms of both intensity and localization. Furthermore, the Actisham protocol shunts the current, preventing it from reaching the cortex (Fig. 2), thus avoiding causing any brain excitability changes.[68]

Outcome Measures

An independent assessor (an assistant research fellow), blinded to the group allocation, collected the outcomes measures.

Primary Outcomes

Measures of Cortical Activity and Connectivity

Measures of cortical activity and connectivity were collected at baseline and immediately after intervention. Resting-state EEG (~10 minutes, eyes closed) was obtained in a quiet room while the participants were sitting upright in a comfortable chair. Participants were asked to refrain from alcohol for 24 hours or caffeinated drinks on the day of recording to avoid alcohol- or caffeine-induced changes in the EEG stream. EEG data were collected using the same transcranial electrical stimulator (Starstim32, Neuroelectrics, Barcelona, Spain). The EEG was sampled with 32 electrodes placed in the standard 10–10 international placement, and impedances were checked to remain <5 kΩ. The EEG data were acquired using NIC2 software (Neuroelectrics, Barcelona, Spain) with a sampling rate of 500 Hz. Data were resampled to 128 Hz, band-pass filtered (fast Fourier transform filter) to 0.01 to 44 Hz, and rereferenced to the average reference using the EEGLAB package in MATLAB (MathWorks, Natick, MA). The data were plotted in EEGLAB and ICoN for a careful inspection and manual rejection of artifacts.

Standardized low-resolution brain electromagnetic tomography (sLORETA), through LORETA-key software, was used to estimate intracerebral electrical sources that generate scalp-recorded electrical activity in each of the following five frequency bands: infraslow (0.01–0.1 Hz), theta (4–7.5 Hz), alpha (8–12 Hz), beta (12.5–30 Hz), and gamma (30.5–44 Hz). These frequencies were chosen because they have been previously reported to be altered in individuals with chronic pain. The following three analyses were used to explore the effects of the HD-tIPNS on cortical activity and connectivity:

- Regions of interest (ROIs) analysis was used to calculate and compare the log-transformed current density changes at the targeted brain regions. The ROI maker 1 function in LORETA was used to define the ROI. A seed point was provided for each ROI, and all voxels within a radius of 10 mm were averaged to calculate the log-transformed current density. The ROIs in this study included the left and right S1 (S1L and S1R), pgACC, and dACC. For the ROIs closer to midline (ie, pgACC and dACC), we do not differentiate between the left and right owing to their proximity to the midline and difficulty in differentiating laterality because of volume conduction.

- Instantaneous connectivity and lagged phase functional connectivity were used as a measure of coherence and were calculated between the targeted brain regions (pgACC, dACC, and S1) for all five frequency bands described earlier.[72–74] Coherence and phase synchronization between time series corresponding to different spatial locations are usually interpreted as indicators of the "functional connectivity." The Connectivity1 function in LORETA-key software was used to calculate the functional connectivity between the targeted ROIs. Measures of linear dependence (coherence) between the multivariate time series are defined. The measures are expressed as the sum of lagged dependence and instantaneous dependence. The measures are nonnegative and take the value zero only when there is independence of the pertinent type. On the basis of this principle, the instantaneous and the lagged linear connectivity were calculated.
- Effective connectivity: Granger causality reflects the strength of effective connectivity (ie, causal interactions) from one region to another by quantifying how much the signal in the seed region can predict the signal in the target region.[75,76] In other words, it can be considered directed functional connectivity. The isolated effective coherence function in LORETA-key software was used to calculate the Granger causality between ROIs. Granger causality is based on formulating a multivariate autoregressive model and calculating the corresponding partial coherences after setting all irrelevant connections to zero.[77] In general, the autoregressive coefficients correspond to Granger causality.[76,78] Granger causality is defined and calculated as the log-ratio between the error variance of a reduced model, which predicts one time series based only on its own past values, and that of the full model, which also includes the past values of another time series. It is important to note that Granger causality does not imply anatomical connectivity between regions but directional functional connectivity between two sources. Given effective connectivity reflects directional functional connectivity, only the frequency bands and the ROIs that showed significant differences in functional connectivity analysis were selected for Granger causality analysis.

Safety Measures

Safety measures were collected immediately before intervention and one day after intervention. The following variables were recorded:

- Qualitative description and intensity of each symptom on a Likert scale (0 = none to 10 = extreme).
- Relation of symptom to treatment, measured on a scale ranging from 1 = unrelated to 5 = strongly related.
- Duration and time taken for resolution of each symptom, expressed in minutes.
- Worsening or improvement of symptoms, using the Discontinuation-Emergent Sign and Symptom (DESS).[79]
- Any withdrawals because of adverse effects.

Secondary Outcomes

Numeric Pain Rating Scales

NPRS were collected at baseline and one day after intervention. An 11-point (0 = not at all to 10 = worst) scale was used individually to evaluate changes in the current pain, and the worst pain, average pain, unpleasantness, bothersomeness, and interference because of pain in the past 24 hours.

Statistical Analysis

SPSS (version 27.0; IBM, Armonk, NY) was used for all statistical analyses. Descriptive statistics were used to summarize safety measures. To adjust for the variability at baseline, percentage changes to baseline were calculated for measures of cortical activity and connectivity and the NPRSs as follows:

$$\text{Percent change to baseline} = \frac{\text{Postintervention} - \text{Preintervention}}{\text{Preintervention}} \times 100$$

Individual tests were conducted for each ROI and the functional connectivity measure in each of the five frequency bands. A Mann-Whitney U test was used to compare the between-group differences in the percentage changes for each outcome measure. A p value of <0.01 was considered significant.

Granger causality was calculated for the functional connectivity measures that showed significant between-group differences. A Wilcoxon signed-rank test was used to identify the difference in the Granger causality measure before and after HD-tIPNS. A p value of <0.05 was considered significant.

RESULTS

Participant Characteristics

A total of 30 participants with CLBP (n = 15 in each group) were enrolled (between November 2021 and January 2022) and randomized equally into two treatment groups. Table 1 presents the descriptive data for all participants at baseline, indicating the two groups were comparable. There were no dropouts. The trial was stopped at the end of January because we reached the desired sample.

Safety

A few participants reported a range of adverse effects, particularly in the Sham group compared with the HD-tIPNS group (Fig. 3). However, these symptoms were mild and short-lived. The most common adverse effect in the HD-tIPNS group was headache and fatigue. No serious adverse events occurred.

Region of Interest

The findings of the ROI analysis are presented in Figure 4. No significant differences were observed between the Sham and the HD-tIPNS in the activity (log-transformed current density) of the pgACC, dACC, S1L, and S1R for any frequency bands (Fig. 3).

Functional Connectivity

Instantaneous Phase Synchronization

A significant decrease in the instantaneous functional connectivity was noted between the pgACC and dACC (U = 47.0, Z = −2.72, p = 0.007) and the pgACC and S1L (U = 41.0, Z = −2.97, p = 0.003) in the infraslow band after HD-tIPNS when compared with sham stimulation (Fig. 5a,b, respectively). No significant differences were observed in the other frequency bands and between other ROIs (Fig. 5c–f).

Table 1. Demographics and Clinical Characteristics of Participants.

Characteristics/measures	Group 1, HD-tIPNS, n = 15	Group 2, Sham, n = 15
Age, y	39.2 ± 16.0	44.6 ± 13.1
Sex		
Female, n (%)	9 (60)	10 (67)
Male, n (%)	6 (40)	5 (33)
Ethnicity		
NZ European, n (%)	11 (73)	10 (67)
Māori, n (%)	3 (20)	3 (20)
Indian, n (%)	1 (7)	1 (7)
Other, n (%)	0 (0)	1 (7)
Employment		
Employed, n (%)	6 (40)	8 (53)
Unemployed, n (%)	1 (7)	4 (27)
Retired, n (%)	1 (7)	1 (7)
Looking after family, n (%)	3 (20)	1 (7)
Self-employed, n (%)	2 (13)	1 (7)
Other, n (%)	2 (13)	0 (0)
Education		
University degree, n (%)	8 (53)	5 (33)
Trade/apprenticeship, n (%)	1 (7)	1 (7)
Certificate/diploma, n (%)	2 (13)	3 (20)
Year 12/equivalent, n (%)	1 (7)	2 (13)
Year 10/equivalent, n (%)	3 (20)	0 (0)
No formal qualification, n (%)	0 (0)	4 (27)
Duration of pain, mean ± SD, y	7.4 ± 9.7	6.6 ± 5.4
Brief Pain Inventory		
Severity, mean ± SD	3.7 ± 1.0	4.4 ± 1.3
Interference, mean ± SD	3.6 ± 2.1	4.9 ± 2.1
Roland-Morris Disability Questionnaire, mean ± SD	11.2 ± 5.1	11.9 ± 4.3
Neuropathic pain, PainDETECT, mean ± SD	10.0 ± 6.2	11.7 ± 6.6
Central sensitization, CSI, mean ± SD	39.3 ± 18.0	45.0 ± 10.0
Well-being, WHO-5	13.3 ± 5.0	12.7 ± 5.1
Quality of life, EQ-5D		
Index score, mean ± SD	0.7 ± 0.1	0.7 ± 0.1
VAS, mean ± SD	69.1 ± 20.3	67.9 ± 16.6
Pain catastrophizing, PCS		
Rumination, mean ± SD	6.9 ± 4.3	7.4 ± 3.4
Magnification, mean ± SD	3.8 ± 2.5	4.7 ± 2.3
Helplessness, mean ± SD	6.9 ± 5.6	8.9 ± 3.7
Total, mean ± SD	17.7 ± 10.7	20.9 ± 8.4
Pain vigilance and awareness, mean ± SD	35.7 ± 15.3	43.9 ± 10.5
Depression, DASS-21, mean ± SD	6.1 ± 4.6	5.9 ± 4.9
Anxiety, DASS-21, mean ± SD	6.2 ± 5.3	4.9 ± 2.8
Stress, DASS-21, mean ± SD	8.9 ± 5.9	6.9 ± 3.2

CSI, central sensitization inventory; DASS-21, depression, anxiety and stress scale; EQ-5D, European Quality of Life-Five Dimensions; PCS, pain catastrophising scale; VAS, visual analogue scale; WHO-5, 5-item World Health Organization Well-Being Index.

Lagged Phase Synchronization

No significant differences were observed in the lagged phase functional connectivity in any of the frequency bands and between any ROIs (Fig. 5g–l).

Effective Connectivity

A significant decrease in the instantaneous effective connectivity was noted in the direction of the dACC to the pgACC ($Z = -2.10$, $p = 0.035$), in the infraslow band after HD-tIPNS when compared with baseline (Fig. 6). No significant differences were observed in the direction of the pgACC and S1L ($Z = -1.846$, $p = 0.066$).

Clinical Measures

Figure 7 presents the violin plots for differences in the clinical measures between HD-tIPNS and sham stimulation. The Mann-Whitney tests revealed no significant between-group differences in any of the pain measures, including current pain, worst pain, average pain, unpleasantness, bothersomeness, and pain interference.

DISCUSSION

One of the primary aims of this study was to evaluate the safety of the novel HD-tIPNS technique. The findings of this study confirm the safety of this novel transcranial stimulation technique for treatment of CLBP. We used an extensive DESS scale to assess the immediate adverse effects of HD-tIPNS. No serious adverse events were reported by any participant. Furthermore, there were no differences in reported adverse effects between real and sham stimulation, except for headache, which appeared somewhat more prevalent in the real stimulation group. The adverse effects reported were mild, transient, and self-resolved after the treatment session. These findings are consistent with previous studies using other transcranial electrical stimulation protocols for chronic pain and in studies using a pink-noise stimulation protocol for food addiction.

One of the main findings of this study is that a transcranially applied novel stimulation design consisting of an infraslow stimulation with embedded pink noise can change functional connectivity in the infraslow frequency band between the key hubs of the three main pain pathways. Furthermore, the transcranially applied stimulation modulates the information flow from the dACC to the pgACC. A previous study showed that in patients with chronic neuropathic pain, the dACC exerts a (likely inhibitory) effect on the pgACC, in contrast to healthy controls, in the alpha band, which can be modulated by spinal cord stimulation.[11] It is known that alpha activity is nested on infraslow activity, as shown from the initial discovery in 1957 of infraslow activity in the thalamus.[80] In this study, we did not observe any effect in the alpha frequency band but found that the novel HD-tIPNS design can modulate the same connection in the infraslow band, potentially exerting a similar effect.

The finding that communication can be altered between the three main hubs of the interacting pain networks suggests that it is worthwhile to verify whether repetitive stimulations can clinically benefit patients with pain syndromes. No clinical benefit was noted in this study after a single stimulation session. This could be attributed to several factors, including methodologic issues, in which the large variability in collected data (violin plots, Fig. 7) prevents observation of statistical significance. However, the means of clinical pain measures were very similar between real and sham stimulation, making this less likely. It is more likely that the absences of clinical benefit may be related to the stimulation per se. It could be that repeated stimulations may be required to induce a clinical benefit, even though a single stimulation already

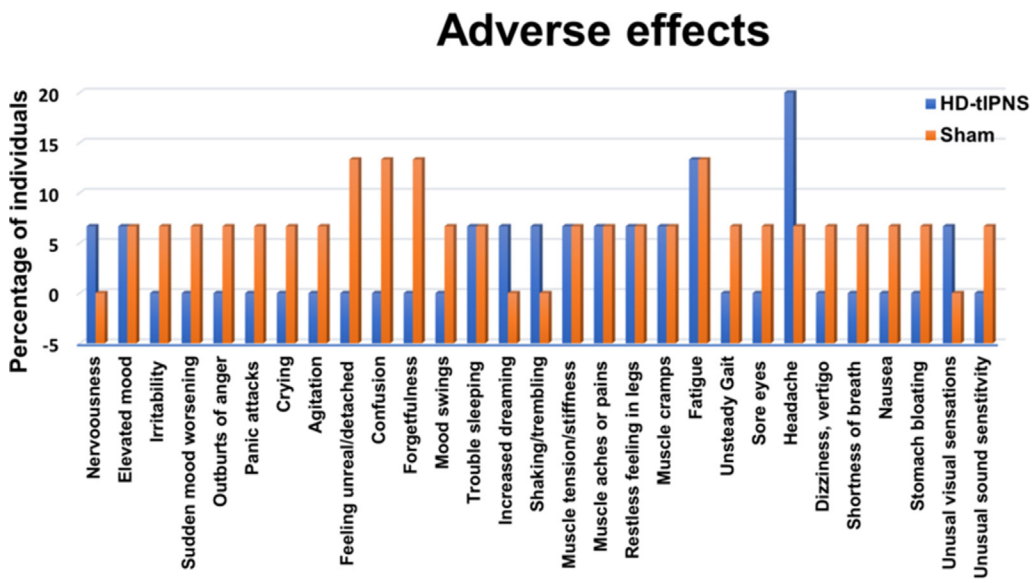

Figure 3. Adverse effects reported immediately after the transcranial electrical stimulation session. [Color figure can be viewed at www.neuromodulationjournal.org]

introduces an electrophysiological change. This is analogous to the finding in a study in which an electrode was implanted in the dACC in people with obsessive compulsive disorder.[81] Here, too, the electrophysiological changes preceded clinical changes.[81] Furthermore, it has been shown that the optimal clinical benefit when targeting the dACC with implants for pain may be delayed for several days,[45,46] suggesting that more stimulation sessions are essential before the patient benefits clinically from the stimulation

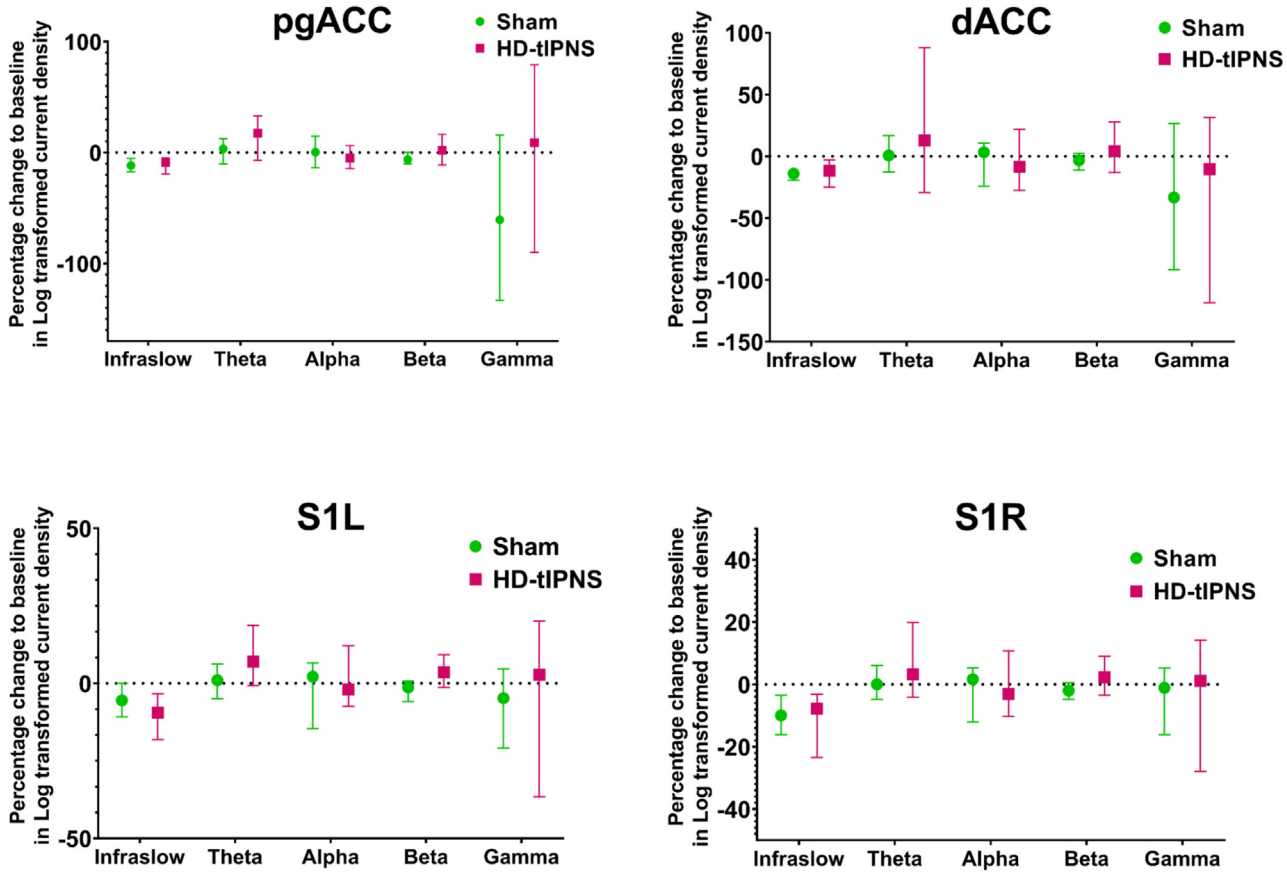

Figure 4. ROI analysis. The Mann-Whitney tests showed no significant between-group differences in the log-transformed current densities at the targeted brain regions. [Color figure can be viewed at www.neuromodulationjournal.org]

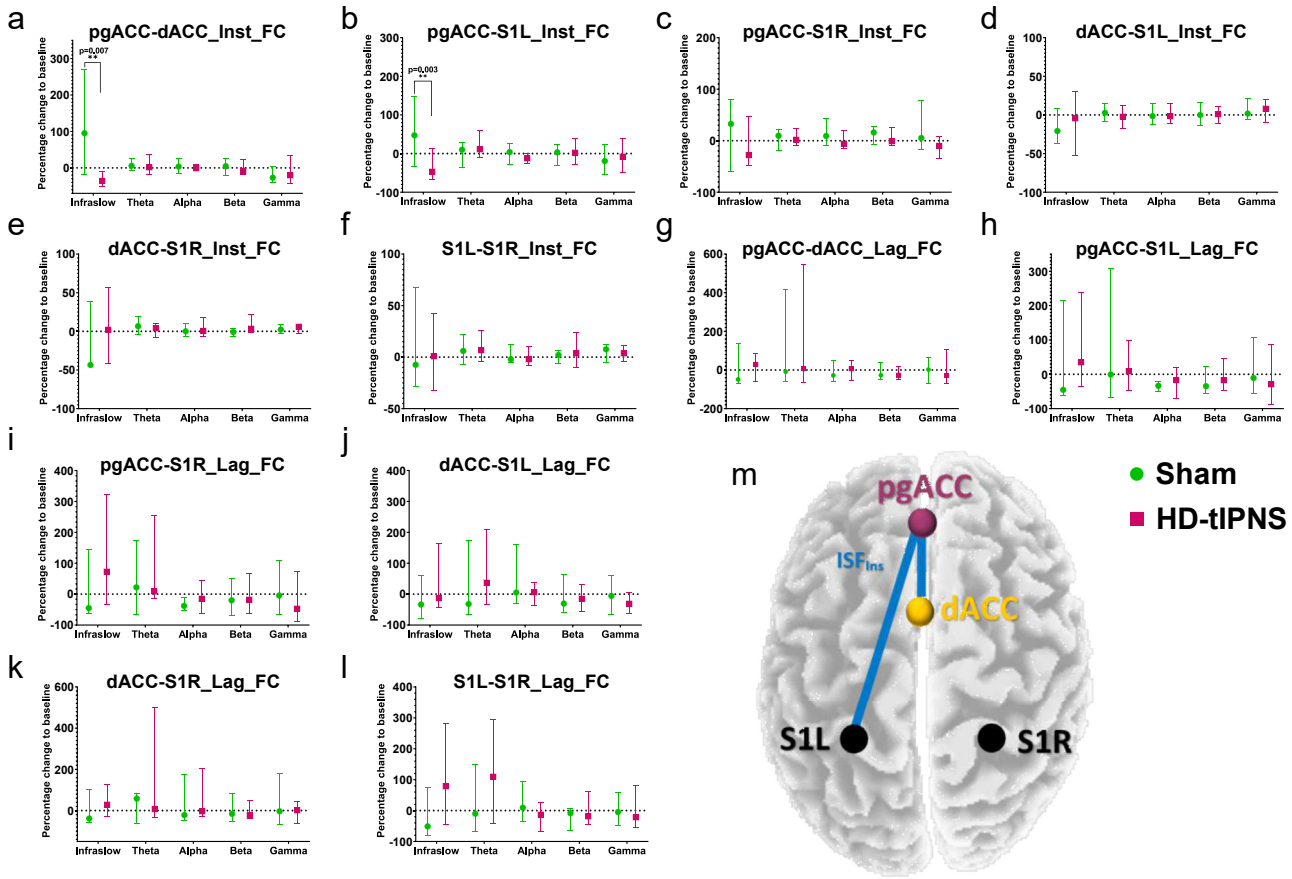

Figure 5. Functional connectivity analysis. a–f. Instantaneous phase synchronization between targeted brain regions. A significant decrease in instantaneous functional connectivity was seen between (a) the pgACC and dACC and (b) the pgACC and S1L after HD-tIPNS when compared with sham stimulation. g–l. Lagged phase synchronization between targeted brain regions. No significant between-group differences were noted in lagged phase synchronization. The symbol shows the median, and the lines show the interquartile range. m. Summary of functional connectivity results, showing decreased functional connectivity between the pgACC and dACC and the pgACC and S1L, after HD-tIPNS. FC, functional connectivity; Inst, instantaneous phase synchronization; ISF, infraslow frequency; Lag, lagged phase synchronization. [Color figure can be viewed at www.neuromodulationjournal.org]

protocol. Another possibility is that the theoretical model is wrong, and that the targets are not optimal. This is unlikely in view of a recent meta-analysis that confirms these targets are indeed relevant for pain.[12] A third possibility is related to the amplitude of the stimulation currents. We used a fixed amplitude, determined by computer simulations designed to determine the amplitude delivered at each stimulation electrode in a fractionated way (Figs. 1 and 2). Considering that each participant's skull has a different

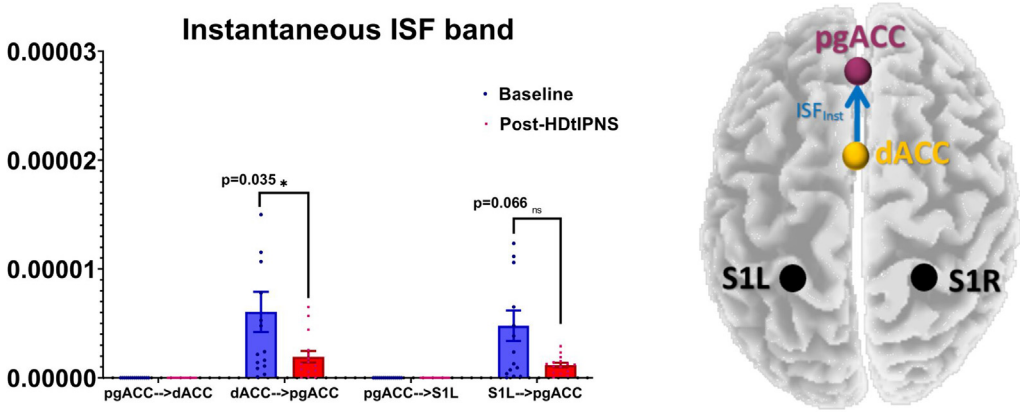

Figure 6. Effectivity connectivity analysis. A significant decrease in the instantaneous effective connectivity was noted in the direction of the dACC to the pgACC in the infraslow band after HD-tIPNS. Although a decrease was noted in the instantaneous effective connectivity in the direction of the S1L to the pgACC, this did not show statistical significance. No significant differences were noted in other effective connectivity (ie, from the pgACC to the dACC or the S1L). The bar shows the mean, and the error bar shows the SEM. ISF, infraslow frequency. [Color figure can be viewed at www.neuromodulationjournal.org]

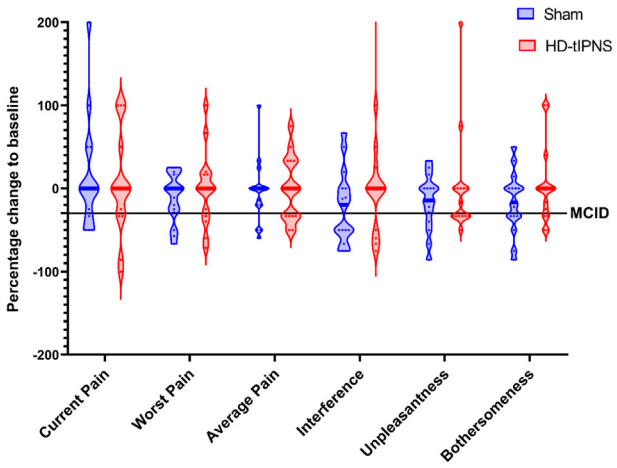

Figure 7. Comparisons of between-group clinical outcomes. MCID, minimal clinical important difference. [Color figure can be viewed at www.neuromodulationjournal.org]

shape and thickness, this may not be optimal. A thicker or thinner skull could result in lower or higher current densities, respectively, at the different targets. This is even more relevant for noise stimulation because this has a stochastic resonance effect and an inverted U-like behavior, meaning that low amplitudes likely exert no effect on the networks, an optimal/intermediate amplitude may strengthen the connectivity and the amplitude of evoked responses, and a very high amplitude may weaken the connectivity and the amplitude of evoked responses.[25,82–84] A fourth possible explanation could be that the ratio of infraslow amplitude to pink noise may also be suboptimal because the pink-noise component may be too weak to exert the desired effect. A fifth reason may be that pink noise may lack power in the higher amplitudes, given pain has been linked to a Bayesian prediction error problem in which predictions about the presence of pain are generated in beta (12–30 Hz) frequencies and prediction errors in gamma frequencies (>30 Hz).[85] Considering that the 1/f noise structure of the brain has the least power in these higher frequency domains, a whiter version of the noise may be better suited to disrupt pathological connectivity than the pink noise, which tries to mimic the innate temporal structure of brain function.[86–88]

One of the primary limitations of this study was the small sample size. A sample size calculation was not performed because this was a pilot exploratory study to evaluate safety and verify whether HD-tIPNS can disrupt functional connectivity between targeted cortical regions. Based on the results of this study, a future full-powered study will be designed to test the efficacy of this novel treatment approach. Another limitation of the study was that a standard montage and current intensity were used for all the participants. Depending on the participant's anatomy (eg, skull shape, thickness), the electric field at the targeted region could be different. Future studies could optimize the montage and adjust the current intensity and amplitude of noise on the basis of individual MRI tractography.

CONCLUSIONS

Infraslow pink-noise stimulation is a novel technique capable of safely modulating functional and effective connectivity in deep brain structures targeted transcranially through fractionated high-density electrical stimulation. Future studies are needed to determine whether repeated sessions of HD-tIPNS also show a clinically meaningful effect for reducing pain and disability in people with chronic pain, by inducing changes in the functional and effective connectivity at the pain-related cortical hubs.

Acknowledgements

The authors thank Ricardo Salvador and Giulio Ruffini from Neuroelectrics for generating the montage and stimulation design used in this study.

Authorship Statements

Divya Bharatkumar Adhia, Dirk De Ridder, Ramakrishnan Mani, John N.J. Reynolds, and Sven Vanneste were responsible for the conceptualization of the study and obtained funding. Divya Bharatkumar Adhia, Dirk De Ridder, Ramakrishnan Mani, John N.J. Reynolds, and Sven Vanneste were responsible for the methods/design of the work. Divya Bharatkumar Adhia and Matthew Hall were responsible for data collection, processing, and analysis. Divya Bharatkumar Adhia and Dirk De Ridder wrote and prepared the original draft. Divya Bharatkumar Adhia, Dirk De Ridder, Ramakrishnan Mani, John N.J. Reynolds, Matthew Hall, and Sven Vanneste wrote, critically reviewed, and revised the manuscript. All authors have critically read and agreed to the final version of the submitted manuscript and agree to be accountable for all aspects of the work.

How to Cite This Article

Adhia D.B., Mani R., Reynolds J.N.J., Hall M., Vanneste S., De Ridder D. 2022. High-Definition Transcranial Infraslow Pink-Noise Stimulation Can Influence Functional and Effective Cortical Connectivity in Individuals With Chronic Low Back Pain: A Pilot Randomized Placebo-Controlled Study.
Neuromodulation 2022; ■: 1–13.

REFERENCES

1. Holland J. *Complexity*. Oxford University Press; 2014.
2. Johnson N. *Simply Complexity: A Clear Guide to Complexity Theory*. 2nd ed. Oneworld Publications; 2010.
3. De Ridder D, Vanneste S, Freeman W. The Bayesian brain: phantom percepts resolve sensory uncertainty. *Neurosci Biobehav Rev*. 2014;44:4–15. https://doi.org/10.1016/j.neubiorev.2012.04.001.
4. Amaral LA, Díaz-Guilera A, Moreira AA, Goldberger AL, Lipsitz LA. Emergence of complex dynamics in a simple model of signaling networks. *Proc Natl Acad Sci U S A*. 2004;101:15551–15555. https://doi.org/10.1073/pnas.0404843101.
5. Bullmore E, Sporns O. The economy of brain network organization. *Nat Rev Neurosci*. 2012;13:336–349. https://doi.org/10.1038/nrn3214.
6. Wikipedia. Emergence. Accessed September 8, 2022. https://en.wikiquote.org/wiki/Emergence.
7. De Ridder D, Vanneste S, Smith M, Adhia D. Pain and the triple network model. *Front Neurol*. 2022;13:757241. https://doi.org/10.3389/fneur.2022.757241.
8. Kong J, Loggia ML, Zyloney C, Tu P, LaViolette P, Gollub RL. Exploring the brain in pain: activations, deactivations and their relation. *Pain*. 2010;148:257–267. https://doi.org/10.1016/j.pain.2009.11.008.
9. Bushnell MC, Ceko M, Low LA. Cognitive and emotional control of pain and its disruption in chronic pain. *Nat Rev Neurosci*. 2013;14:502–511. https://doi.org/10.1038/nrn3516.

10. Price DD. Psychological and neural mechanisms of the affective dimension of pain. *Science*. 2000;288:1769–1772.
11. Vanneste S, De Ridder D. Chronic pain as a brain imbalance between pain input and pain suppression. *Brain Commun*. 2021;3:fcab014.
12. De Ridder D, Adhia D, Vanneste S. The anatomy of pain and suffering in the brain and its clinical implications. *Neurosci Biobehav Rev*. 2021;130:125–146.
13. Baliki MN, Petre B, Torbey S, et al. Corticostriatal functional connectivity predicts transition to chronic back pain. *Nat Neurosci*. 2012;15:1117–1119.
14. Coppieters I, Meeus M, Kregel J, et al. Relations between brain alterations and clinical pain measures in chronic musculoskeletal pain: a systematic review. *J Pain*. 2016;17:949–962.
15. Hashmi JA, Baliki MN, Huang L, et al. Shape shifting pain: chronification of back pain shifts brain representation from nociceptive to emotional circuits. *Brain*. 2013;136:2751–2768.
16. Hemington KS, Rogachov A, Cheng JC, et al. Patients with chronic pain exhibit a complex relationship triad between pain, resilience, and within- and cross-network functional connectivity of the default mode network. *Pain*. 2018;159:1621–1630.
17. Kim J, Mawla I, Kong J, et al. Somatotopically specific primary somatosensory connectivity to salience and default mode networks encodes clinical pain. *Pain*. 2019;160:1594–1605.
18. Kong J, Spaeth RB, Wey HY, et al. S1 is associated with chronic low back pain: a functional and structural MRI study. *Mol Pain*. 2013;9:43.
19. Ossipov MH, Morimura K, Porreca F. Descending pain modulation and chronification of pain. *Curr Opin Support Palliat Care*. 2014;8:143–151.
20. Tu Y, Jung M, Gollub RL, et al. Abnormal medial prefrontal cortex functional connectivity and its association with clinical symptoms in chronic low back pain. *Pain*. 2019;160:1308–1318.
21. De Ridder D, De Mulder G, Verstraeten E, Sunaert S, Moller A. Somatosensory cortex stimulation for deafferentation pain. *Acta Neurochir Suppl*. 2007;97:67–74.
22. De Ridder D, Perera S, Vanneste S. State of the art: novel applications for cortical stimulation. *Neuromodulation*. 2017;20:206–214. https://doi.org/10.1111/ner.12593.
23. De Ridder D, Vanneste S, Van Laere K, Menovsky T. Chasing map plasticity in neuropathic pain. *World Neurosurg*. 2013;80:901.e1–901.e5. https://doi.org/10.1016/j.wneu.2012.12.009.
24. Leong SL, De Ridder D, Vanneste S, Sutherland W, Ross S, Manning P. High definition transcranial pink noise stimulation of anterior cingulate cortex on food craving: an explorative study. *Appetite*. 2018;120:673–678. https://doi.org/10.1016/j.appet.2017.10.034.
25. De Ridder D, Maciaczyk J, Vanneste S. The future of neuromodulation: smart neuromodulation. *Expert Rev Med Devices*. 2021;18:307–317. https://doi.org/10.1080/17434440.2021.1909470.
26. Buzsáki G, Mizuseki K. The log-dynamic brain: how skewed distributions affect network operations. *Nat Rev Neurosci*. 2014;15:264–278. https://doi.org/10.1038/nrn3687.
27. Buzsáki G, Draguhn A. Neuronal oscillations in cortical networks. *Science*. 2004;304:1926–1929. https://doi.org/10.1126/science.1099745.
28. Brandl F, Weise B, Mulej Bratec S, et al. Common and specific large-scale brain changes in major depressive disorder, anxiety disorders, and chronic pain: a transdiagnostic multimodal meta-analysis of structural and functional MRI studies. *Neuropsychopharmacology*. 2022;47:1071–1080. https://doi.org/10.1038/s41386-022-01271-y.
29. Baliki MN, Geha PY, Apkarian AV, Chialvo DR. Beyond feeling: chronic pain hurts the brain, disrupting the default-mode network dynamics. *J Neurosci*. 2008;28:1398–1403. https://doi.org/10.1523/JNEUROSCI.4123-07.2008.
30. Baliki MN, Mansour AR, Baria AT, Apkarian AV. Functional reorganization of the default mode network across chronic pain conditions. *PLoS One*. 2014;9:e106133. https://doi.org/10.1371/journal.pone.0106133.
31. Cauda F, Sacco K, Duca S, et al. Altered resting state in diabetic neuropathic pain. *PLoS One*. 2009;4:e4542. https://doi.org/10.1371/journal.pone.0004542.
32. Grooms JK, Thompson GJ, Pan WJ, et al. Infraslow electroencephalographic and dynamic resting state network activity. *Brain Connect*. 2017;7:265–280. https://doi.org/10.1089/brain.2017.0492.
33. Thompson GJ, Pan WJ, Magnuson ME, Jaeger D, Keilholz SD. Quasi-periodic patterns (QPP): large-scale dynamics in resting state fMRI that correlate with local infraslow electrical activity. *Neuroimage*. 2014;84:1018–1031. https://doi.org/10.1016/j.neuroimage.2013.09.029.
34. Agulhon C, Petravicz J, McMullen AB, et al. What is the role of astrocyte calcium in neurophysiology? *Neuron*. 2008;59:932–946. https://doi.org/10.1016/j.neuron.2008.09.004.
35. Alshelh Z, Di Pietro F, Youssef AM, et al. Chronic neuropathic pain: it's about the rhythm. *J Neurosci*. 2016;36:1008–1018. https://doi.org/10.1523/JNEUROSCI.2768-15.2016.
36. Pirttimaki TM, Sims RE, Saunders G, Antonio SA, Codadu NK, Parri HR. Astrocyte-mediated neuronal synchronization properties revealed by false gliotransmitter release. *J Neurosci*. 2017;37:9859–9870. https://doi.org/10.1523/JNEUROSCI.2761-16.2017.
37. Semyanov A, Henneberger C, Agarwal A. Making sense of astrocytic calcium signals — from acquisition to interpretation. *Nat Rev Neurosci*. 2020;21:551–564. https://doi.org/10.1038/s41583-020-0361-8.
38. Albert R, Jeong H, Barabasi AL. Error and attack tolerance of complex networks. *Nature*. 2000;406:378–382. https://doi.org/10.1038/35019019.
39. Bittar RG, Kar-Purkayastha I, Owen SL, et al. Deep brain stimulation for pain relief: a meta-analysis. *J Clin Neurosci*. 2005;12:515–519. https://doi.org/10.1016/j.jocn.2004.10.005.
40. Farrar JT, Young Jr JP, LaMoreaux L, Werth JL, Poole MR. Clinical importance of changes in chronic pain intensity measured on an 11-point numerical pain rating scale. *Pain*. 2001;94:149–158. https://doi.org/10.1016/S0304-3959(01)00349-9.
41. Roland M, Morris R. A study of the natural history of low-back pain. Part II: development of guidelines for trials of treatment in primary care. *Spine*. 1983;8:145–150.
42. Roland M, Morris R. A study of the natural history of back pain. Part I: development of a reliable and sensitive measure of disability in low-back pain. *Spine (Phila Pa 1976)*. 1983;8:141–144. https://doi.org/10.1097/00007632-198303000-00004.
43. Dionne CE, Dunn KM, Croft PR, et al. A consensus approach toward the standardization of back pain definitions for use in prevalence studies. *Spine*. 2008;33:95–103.
44. Grotle M, Brox JI, Vøllestad NK. Concurrent comparison of responsiveness in pain and functional status measurements used for patients with low back pain. *Spine*. 2004;29:E492–E501.
45. Treede RD, Rief W, Barke A, et al. A classification of chronic pain for ICD-11. *Pain*. 2015;156:1003–1007.
46. Neblett R, Cohen H, Choi Y, et al. The Central Sensitization Inventory (CSI): establishing clinically significant values for identifying central sensitivity syndromes in an outpatient chronic pain sample. *J Pain*. 2013;14:438–445. https://doi.org/10.1016/j.jpain.2012.11.012.
47. Mayer TG, Neblett R, Cohen H, et al. The development and psychometric validation of the central sensitization inventory. *Pain Pract*. 2012;12:276–285. https://doi.org/10.1111/j.1533-2500.2011.00493.x.
48. Freynhagen R, Tölle TR, Gockel U, Baron R. The painDETECT project — far more than a screening tool on neuropathic pain. *Curr Med Res Opin*. 2016;32:1033–1057.
49. Parkitny L, McAuley JH, Walton D, et al. Rasch analysis supports the use of the depression, anxiety, and stress scales to measure mood in groups but not in individuals with chronic low back pain. *J Clin Epidemiol*. 2012;65:189–198. https://doi.org/10.1016/j.jclinepi.2011.05.010.
50. Osman A, Barrios FX, Gutierrez PM, Kopper BA, Merrifield T, Grittmann L. The Pain Catastrophizing Scale: further psychometric evaluation with adult samples. *J Behav Med*. 2000;23:351–365. https://doi.org/10.1023/a:1005548801037.
51. Wertli MM, Eugster R, Held U, Steurer J, Kofmehl R, Weiser S. Catastrophizing—a prognostic factor for outcome in patients with low back pain: a systematic review. *Spine J*. 2014;14:2639–2657. https://doi.org/10.1016/j.spinee.2014.03.003.
52. Roelofs J, Peters ML, McCracken L, Vlaeyen JWS. The pain vigilance and awareness questionnaire (PVAQ): further psychometric evaluation in fibromyalgia and other chronic pain syndromes. *Pain*. 2003;101:299–306. https://doi.org/10.1016/S0304-3959(02)00338-X.
53. Ruffini G, Fox MD, Ripolles O, Miranda PC, Pascual-Leone A. Optimization of multifocal transcranial current stimulation for weighted cortical pattern targeting from realistic modeling of electric fields. *Neuroimage*. 2014;89:216–225.
54. Straudi S, Buja S, Baroni A, et al. The effects of transcranial direct current stimulation (tDCS) combined with group exercise treatment in subjects with chronic low back pain: a pilot randomized control trial. *Clin Rehabil*. 2018;32:1348–1356. https://doi.org/10.1177/0269215518777881.
55. Schabrun SM, Jones E, Elgueta Cancino EL, Hodges PW. Targeting chronic recurrent low back pain from the top-down and the bottom-up: a combined transcranial direct current stimulation and peripheral electrical stimulation intervention. *Brain Stimul*. 2014;7:451–459. https://doi.org/10.1016/j.brs.2014.01.058.
56. Schabrun SM, Burns E, Thapa T, Hodges P. The response of the primary motor cortex to neuromodulation is altered in chronic low back pain: a preliminary study. *Pain Med*. 2018;19:1227–1236. https://doi.org/10.1093/pm/pnx168.
57. Ouellette AL, Liston MB, Chang WJ, Walton DM, Wand BM, Schabrun SM. Safety and feasibility of transcranial direct current stimulation (tDCS) combined with sensorimotor retraining in chronic low back pain: a protocol for a pilot randomised controlled trial. *BMJ Open*. 2017;7:e013080. https://doi.org/10.1136/bmjopen-2016-013080.
58. O'Connell NE, Cossar J, Marston L, et al. Transcranial direct current stimulation of the motor cortex in the treatment of chronic nonspecific low back pain: a randomized, double-blind exploratory study. *Clin J Pain*. 2013;29:26–34. https://doi.org/10.1097/AJP.0b013e318247ec09.
59. Mariano TY, Burgess FW, Bowker M, et al. Transcranial direct current stimulation for affective symptoms and functioning in chronic low back pain: a pilot double-blinded, randomized, placebo-controlled trial. *Pain Med*. 2019;20:1166–1177. https://doi.org/10.1093/pm/pny188.
60. Luedtke K, Rushton A, Wright C, et al. Effectiveness of transcranial direct current stimulation preceding cognitive behavioural management for chronic low back pain: sham controlled double blinded randomised controlled trial. *BMJ*. 2015;350:h1640. https://doi.org/10.1136/bmj.h1640.
61. Larie MS, Esfandiarpour F, Riahi F, Derisfard F, Parnianpour M. Effects of cortical and peripheral electrical stimulation on brain activity in individuals with chronic low back pain. *PTJ*. 2019;9:39–46. https://doi.org/10.32598/PTJ.9.1.39.
62. Jafarzadeh A, Ehsani F, Yosephi MH, Zoghi M, Jaberzadeh S. Concurrent postural training and M1 anodal transcranial direct current stimulation improve postural impairment in patients with chronic low back pain. *J Clin Neurosci*. 2019;68:224–234. https://doi.org/10.1016/j.jocn.2019.07.017.

63. Hazime FA, Baptista AF, de Freitas DG, et al. Treating low back pain with combined cerebral and peripheral electrical stimulation: a randomized, double-blind, factorial clinical trial. *Eur J Pain*. 2017;21:1132–1143. https://doi.org/10.1002/ejp.1037.
64. Ahn S, Prim JH, Alexander ML, McCulloch KL, Fröhlich F. Identifying and engaging neuronal oscillations by transcranial alternating current stimulation in patients with chronic low back pain: a randomized, crossover, double-blind, sham-controlled pilot study. *J Pain*. 2019;20:277.e1–277.e11. https://doi.org/10.1016/j.jpain.2018.09.004.
65. Lefaucheur JP, Antal A, Ayache SS, et al. Evidence-based guidelines on the therapeutic use of transcranial direct current stimulation (tDCS). *Clin Neurophysiol*. 2017;128:56–92.
66. Nikolin S, Huggins C, Martin D, Alonzo A, Loo CK. Safety of repeated sessions of transcranial direct current stimulation: a systematic review. *Brain Stimul*. 2018;11:278–288.
67. Woods AJ, Antal A, Bikson M, et al. A technical guide to tDCS, and related non-invasive brain stimulation tools. *Clin Neurophysiol*. 2016;127:1031–1048.
68. Neri F, Mencarelli L, Menardi A, et al. A novel tDCS sham approach based on model-driven controlled shunting. *Brain Stimul*. 2020;13:507–516.
69. Ruffini G, Wendling F, Merlet I, et al. Transcranial current brain stimulation (tCS): models and technologies. *IEEE Trans Neural Syst Rehabil Eng*. 2013;21:333–345.
70. Ruffini G, Wendling F, Sanchez-Todo R, Santarnecchi E. Targeting brain networks with multichannel transcranial current stimulation (tCS). *Current Opinion in Biomedical Engineering*. 2018;8:70–77.
71. Dagan M, Herman T, Harrison R, et al. Multitarget transcranial direct current stimulation for freezing of gait in Parkinson's disease. *Mov Disord*. 2018;33:642–646.
72. Pascual-Marqui RD. Standardized low-resolution brain electromagnetic tomography (sLORETA): technical details. *Methods Find Exp Clin Pharmacol*. 2002;24(suppl D):5–12.
73. Nichols TE, Holmes AP. Nonparametric permutation tests for functional neuroimaging: a primer with examples. *Hum Brain Mapp*. 2002;15:1–25.
74. Pascual-Marqui RD. Discrete, 3D distributed, linear imaging methods of electric neuronal activity. Part 1: exact, zero error localization. Preprint. Posted online October 17, 2007. arXiv 0710.3341. doi:10.48550/arXiv.0710.3341
75. Geweke J. Measurement of linear dependence and feedback between multiple time series. *J Am Stat Assoc*. 1982;77:304–313.
76. Granger CWJ. Investigating causal relations by econometric models and cross-spectral methods. *Econometrica*. 1969;37:424–438.
77. Pascual-Marqui RD, Biscay RJ, Bosch-Bayard J, et al. Assessing direct paths of intracortical causal information flow of oscillatory activity with the isolated effective coherence (iCoh). *Front Hum Neurosci*. 2014;8:448.
78. Valdes-Sosa PA, Roebroeck A, Daunizeau J, Friston K. Effective connectivity: influence, causality and biophysical modeling. *Neuroimage*. 2011;58:339–361.
79. Rosenbaum JF, Fava M, Hoog SL, Ascroft RC, Krebs WB. Selective serotonin reuptake inhibitor discontinuation syndrome: a randomized clinical trial. *Biol Psychiatry*. 1998;44:77–87.
80. Aladjalova NA. Infra-slow rhythmic oscillations of the steady potential of the cerebral cortex. *Nature*. 1957;179:957–959. https://doi.org/10.1038/179957a0.
81. De Ridder D, Leong SL, Manning P, Vanneste S, Glue P. Anterior cingulate implant for obsessive-compulsive disorder. *World Neurosurg*. 2017;97754.e7–754.e16. https://doi.org/10.1016/j.wneu.2016.10.046.
82. Mabil P, Huidobro N, Torres-Ramirez O, et al. Noisy light augments the Na+ current in somatosensory pyramidal neurons of optogenetic transgenic mice. *Front Neurosci*. 2020;14:490.
83. Remedios L, Mabil P, Flores-Hernández J, et al. Effects of short-term random noise electrical stimulation on dissociated pyramidal neurons from the cerebral cortex. *Neuroscience*. 2019;404:371–386.
84. Huidobro N, Gutierrez-Gomez A, Gutierrez J, et al. Augmenting global coherence in EEG signals with binaural or monaural noises. *Brain Topogr*. 2020;33:461–476.
85. De Ridder D, Vanneste S. The Bayesian brain in imbalance: medial, lateral and descending pathways in tinnitus and pain: a perspective. *Prog Brain Res*. 2021;262:309–334. https://doi.org/10.1016/bs.pbr.2020.07.012.
86. De Ridder D, Vanneste S, Plazier M, Vancamp T. Mimicking the brain: evaluation of St Jude Medical's Prodigy Chronic Pain System with Burst Technology. *Expert Rev Med Devices*. 2015;12:143–150. https://doi.org/10.1586/17434440.2015.985652.
87. Strube A, Rose M, Fazeli S, Büchel C. The temporal and spectral characteristics of expectations and prediction errors in pain and thermoception. *Elife*. 2021;10. https://doi.org/10.7554/eLife.62809.
88. Nickel MM, Tiemann L, Hohn VD, et al. Temporal-spectral signaling of sensory information and expectations in the cerebral processing of pain. *Proc Natl Acad Sci U S A*. 2022;119. https://doi.org/10.1073/pnas.2116616119.